Chapter 8

Variations of the harmonic components of the X-ray Pulse Profile of PSR B1509-58[1]

8.1 Introduction

With several sensitive space missions in the last two decades, the detection of rotation-powered pulsars observable at X-ray energies has increased substantially. Pulsars with ages ranging from 10^3 - 7×10^9 years, magnetic field strength ranging from 10^8 - 10^{13} G and spin periods ranging from 1.6 ms - 530 ms have been detected in the X-rays [432].

Owing to their fast rotation periods, magnetic fields of millisecond and young pulsars

[1]Based on the paper 'Variations of the harmonic components of the X-ray Pulse Profile of PSR B1509-58' in RAA Vol 15 No. 1 (2015)

at their respective light cylinders are comparable even though the surface magnetic fields of the young pulsars are nearly five orders of magnitude larger than those of the former. This suggests to us that the magnetic field strength at the light cylinder may play a role in high energy emission in pulsars [433].

In young pulsars with ages less than 2000 years like the Crab pulsar, magnetospheric emission from charged particles accelerated in the neutron star magnetosphere along the curved magnetic field lines (outer gap model) dominate [75]. The magnetospheric component at X-ray energies is characterized by strong pulsations, sometimes with several peaked structure [432]. Asymmetric pulse shapes indicate lack of axial symmetry in the emission zone. In millisecond pulsars like PSR 1821-24, PSR B1937+21, and PSR J0218+4232, the X-ray emission is dominated by non-thermal processes [432]. Their pulse profiles have narrow peaks and high pulsed fraction.

PSR B1509-58 was discovered in X-rays by the *Einstein* satellite [434], and later observations in radio [435] confirmed its 150 ms period and the highest spin-down rate of $\dot{P} \sim 1.5\times\ 10^{-12}$ s s^{-1} of any known pulsar. It has a characteristic age nearly 1700 years, spin-down luminosity of $\dot{E}$ = 1.7 $\times$ 10^{37} erg s^{-1} , and dipole magnetic field of 1.5 $\times$ 10^{13} G. This magnetic field is larger than the magnetar SGR 0418+5729 having the smallest magnetic field less than 7.5 $\times$ 10^{12} G [436]. Further, its braking index, n is less than 3 i.e.,2.839 $\pm$ 0.003 [437]. This could be due to the magnetic field being non-dipolar [438], or a result of pulsar wind that carries particles taking angular momentum away from the pulsar causing resultant mass loss [439]. Some other reasons could be having a time variable effective magnetic moment [440] or the torque function defined by K = - $\dot{\Omega}/\Omega^n$ where Ω is the spin rate of pulsar, being time varying [441].

PSR B1509-58 has been observed regularly since 1996 till 2011 with the Proportional Counter Array (PCA) [87, 442] on board the Rossi X-ray Timing Explorer (*RXTE*). No glitches from this source have been observed so far hence it gives us an opportunity to study the basic emission properties of this source over a long time without interruption. Also no magnetar like X-ray bursts were discovered in this pulsar.

Previous works on this pulsar showed that the X-ray component lags the radio component of the pulse by ~ 0.27 period. The phase relation between the radio and the X-ray pulses, i.e, the arrival time difference between the radio and the X-ray pulses have been found to be quite stable [443]. This lag is energy independent for the range 2-100 KeV [444] suggesting that the radio and X-ray emission regions are different favouring the outer gap model. This pulsar is known to emit radiations from radio to soft-gamma region suggesting that there may be new class of pulsars called soft-gamma ray pulsars [445].

The timing studies of radio pulsars reveal that they are subjected to a systematic delay or spinning down. The measurements of the first and second time derivatives of pulsars spin period can provide us useful information about the dynamics of rotation of non-accreting neutron stars. The timing residuals for PSR B1509-58 from 1996-2010 shows some significant structure. Also while the braking index n is stable at long time scales, its variabilty is visible in short time scales [437]. This could well be due to changes in the magnetospheric activities of this pulsar which may produce corresponding changes in the high energy X-ray emission. For PSR B1509-58, no variability in X-ray flux nor any pulse profile variability has been found when the pulse profiles were compared by a χ^2 test, while upper limits of 28 % was obtained in flux change [437].

In this work we present our analysis of fifteen years of archival data of PSR B1509-58 observed using *RXTE*. The next Section gives the details of the observations and the analysis techniques used; followed by Section 8.3 where we present the results. We then conclude with discussions on the obtained results.

8.2 Observation and data analysis

RXTE was launched on December 30, 1995. It comprised of two pointed instruments, the Proportional Counter Array (PCA) in the energy range 2-60 KeV and the High Energy X-ray Timing Experiment (HEXTE) covering the higher energy range 15-250 KeV. In addition, *RXTE* carried an All-Sky Monitor (ASM) that scanned the sky. We used data obtained with the Proportional Counter Array (PCA) [87]. PCA is a collimated array of proportional counters, and is composed of 5 Proportional Counter Units (PCUs) with a total photon collection area of 6500 cm^2. Over the years, the average number of detectors available for observation decreased and the mission ended in early 2012. For PSR B1509-58, archived *RXTE*-PCA data are available for 15 years from 1996 to 2011 which enables us to study its timing characteristics in detail. We used data in Good Xenon mode that provides a full timing accuracy of about 1 μs. From the Science Event files recorded in Good Xenon mode, light curves were created using `seextrct` with a binning of 10 ms. The exposure for the 262 observations used for this analysis were typically of the order of kilo seconds. Barycentric corrections were then made on the light curve so created using `faxbary`. Using the `FTOOLS` task `efsearch`, we find the best pulse period for each of the barycenter corrected light curves. One such period search is shown in Figure 8.1. Pulse profiles with 128 phase bins were created by folding the light curves with their respective best periods determined with a resolution of 10^{-7} s. In order to choose the appropriate energy range, we first searched for channel range with the maximum signal to noise ratio. The light curves were extracted for different energy intervals for a 1996 observation and the respective pulse profiles were created. Each profile was fitted with a constant and the χ^2 value was noted. The greater is the deviation, the larger is the value of χ^2, and hence greater is the signal to noise ratio. This way the channel and hence energy range is optimised for further analysis. The channel range optimisation plot is given in Figure 8.2. The pulse profiles were created for all the 262 observations taking the energy range to be 2 to 24 KeV. A sample pulse profile is given in Figure 8.3.

Next, Fourier decomposition of the pulse profiles were carried out. The Fast Fourier Transform (FFT) method will decompose the signal from the pulsar into Fourier components and we get the amplitudes and phases of the frequency components the sum of which make the individual pulse profiles. It is then possible to calculate the relative amplitudes and the phase differences of the harmonics with respect to the fundamental for the pulse profile of all the years. Should the pulse profile remain unchanged the the relative amplitudes and phases of the harmonics with respect to the fundamental will be constant over time and will establish the hypothesis that this pulsar has stable X-ray properties on long time scales.

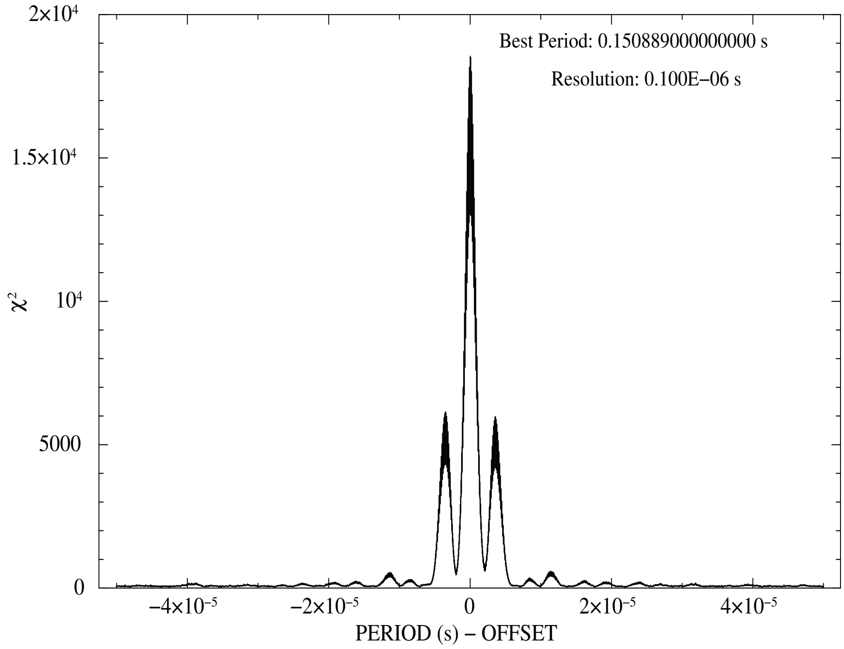

Figure 8.1: The χ^2 in the pulse profile for PSR B1509-58 for different trial pulse period is plotted here for a sample observation with *RXTE*-PCA data. The peak represents the true period.

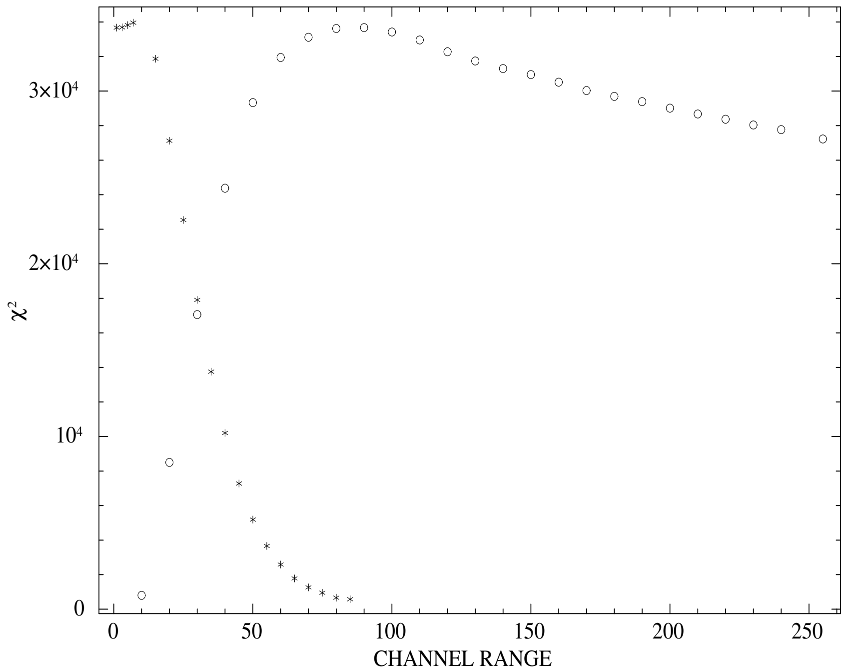

Figure 8.2: Plot for optimisation of channel range for pulse profile extraction of PSR B1509-58 with *RXTE*-PCA data. The χ^2 of the folded light curve is plotted here for different channel ranges. For the circles, the X-axis represents the highest channel while the lowest channel is set to zero. This curve stops rising at about channel no 90. For the asterisks, the X-axis represents the lowest channel when the highest channel is fixed at 90. A channel range of 3-80 was selected for further analysis which will give highest signal to noise ratio in the pulse profile.

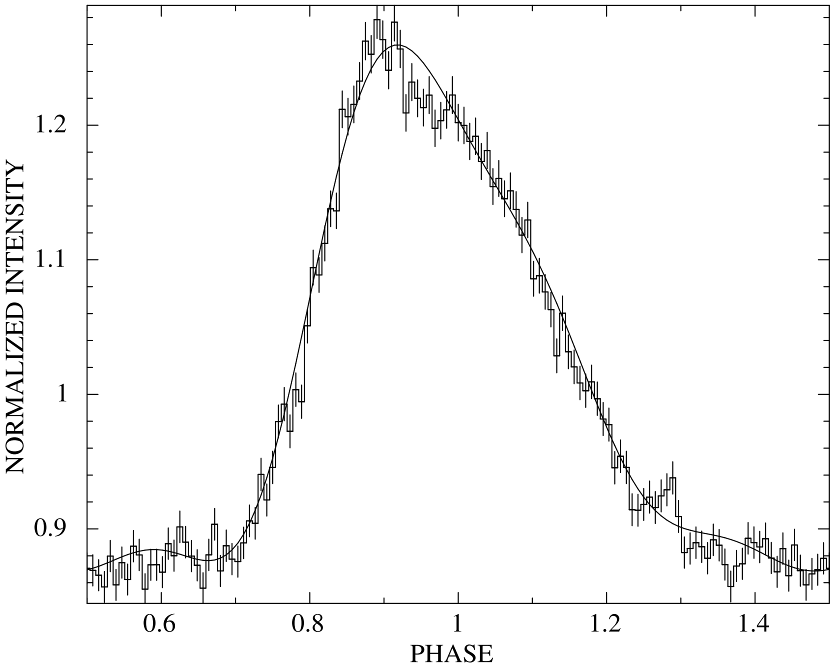

Figure 8.3: A sample pulse profile of PSR B1509-58 in the energy range 2-24 KeV. The pulse profile reconstructed by using the fundamental and the first three harmonics is overlayed.

Since the pulse profiles have limited statistics, there are definite uncertainties with the measurement of the amplitudes and the phases. We have decomposed the individual pulse profiles into 128 Fourier components. In our analysis, we see that the first four Fourier components have the largest amplitudes and therefore have small relative errors and are hence the most significant components. We compare only these significant Fourier components. This is depicted in Figures 8.4 & 8.5. Hence we make a comparison of the relative amplitudes and phase differences of the first three harmonics with respect to the fundamental. To make a comparison of phases, first the fundamental is shifted to zero, by subtracting it from itself. The first harmonic is shifted by twice the fundamental, second harmonic by thrice and the third harmonic by four times that. This way the phase differences between the first, second and third harmonic and the fundamental is determined. We also calculate the ratio of the amplitudes of the first three harmonics with respect to the fundamental.

8.3 Results

The relative amplitudes of the first,second and third harmonics and their fundamental for all the observations are shown in Figure 8.6 and the phase differences of the first three harmonics with respect to the fundamental in Figure 8.7. The long term average amplitudes of the first, second and third harmonics (and their standard deviation for individual measurements) compared to the fundamental are 36.9 % (1.7 %), 13.4 % (1.9 %) and 9.4 % (1.8 %) respectively. Similarly, the phases of the three harmonics (and standard deviations) with respect to the fundamental are 0.36 (0.06), 1.5 (0.2), 2.5 (0.3) radian respectively.

To calculate the errors on the measured amplitudes and phases of the harmonics we have carried out a Monte Carlo simulation. Pulse profiles were simulated with an intrinsic profile same as that shown with the solid line in Figure 8.3 but with a Gaussian deviation in each bin due to limited photon statistics. The same parameters were then measured from the simulated pulse profiles. The process was carried out 10,000 times and the standard deviation of each of the parameters obtained from the 10,000 simulations was taken to be the error on that parameter. The error obtained in a given pulse profile however depends on the total number of photons used to create the pulse profile. We have therefore estimated the dependence of the errors on the total number of photons used to create the pulse profiles by repeating the process for different number of total photons. As expected, a power-law dependence with index -1/2 was found between the errors and the total number of photons. The total number of X-ray photons, which is known for each of the observations was then used along with the above results to determine the error of the parameters for each of the observations. It was however found that there is a larger scatter in the measured parameters around the mean value compared to those obtained from the Monte Carlo simulation. We have measured the standard deviation of the parameters obtained from the 25 observations carried out in 2004 and obtained a scaling between the scatter and the errors estimated from the Monte Carlo simulation. All the error bars were multiplied by this scaling factor and are shown in Figures 8.6 and 8.7.

To investigate if there is an underlying trend, we have overplotted a nine point running average for each of the plots. The running mean indicates that on a longer timescale of about a year, there could be some systematic variation in the pulse profiles with upper limit on percentage variation of the relative amplitudes of the first three harmonics to the fundamental being within 4 %, 13 % and 17 % and phases differences of first three harmonics from the fundamental being within 0.05, 0.15 and 0.14 radian of the respective long term averages. From Figures 8.6 and 8.7, it is also evident that there is a greater variation of phase difference and relative amplitudes for the later years data of *RXTE* from the mean. This is probably due to the reduced sensitivity of the PCA resulting from loss of PCUs in the subsequent years of operation.

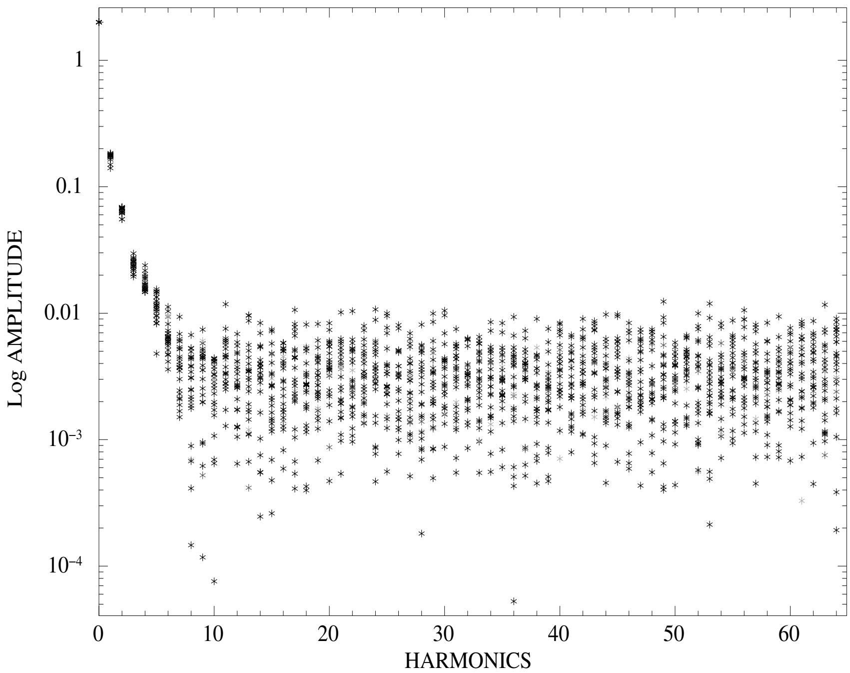

Figure 8.4: Amplitudes of the harmonics of the pulse profiles for PSR B1509-58 are plotted here for 25 pulse profiles obtained from observations in 2004.

8.4 Discussion

Pulsars show many types of flux variation on different time scales. The short term flux variation being bursts [446] and glitches [447]. No glitches has been observed for PSR B1509-58 while the younger Crab pulsar had 24 glitches in 42 years [448] implying that the former has a higher internal temperature than the latter [449]. Unlike the Crab and the Vela pulsar, PSR B1509-58 exhibits only an asymmetric, broad X-ray pulse suggesting that X-ray pulse emission region is closer to neutron star for PSR B1509-58 than for the other two [450]. The pulse profile analysis of PSR B1509-58 done here for the observations during the years 1996–2011 indicate some scatter in the amplitudes and phases. This is however not detectable by eye on pulse profiles.

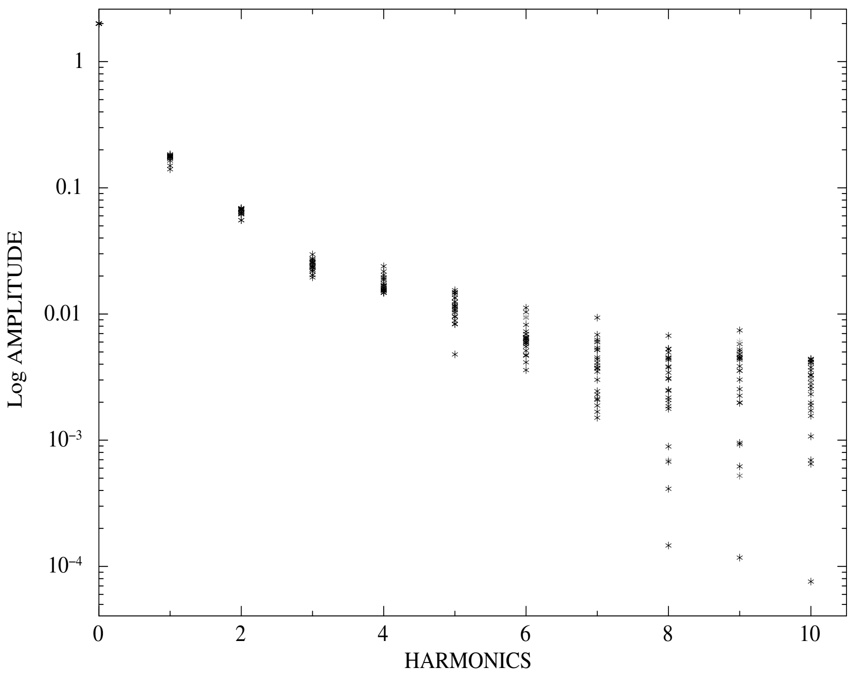

Figure 8.5: Same as Figure 8.4, only the first 10 harmonics are shown here.

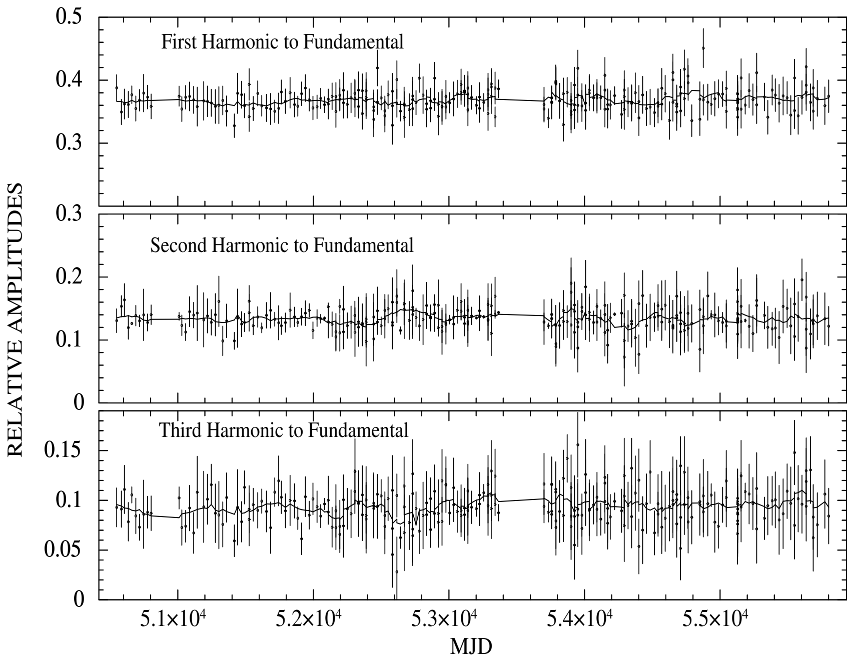

Figure 8.6: The line represents the running mean over nine points of the relative amplitudes of the first three harmonics for the pulse profile of PSR B1509-58 with respect to the fundamental while the points represent the actual values. The X-axis represents the MJD. The error bars were determined using the total number of photons in each pulse profile, results from a Monte Carlo simulation of the profiles and a scaling factor described in Section 8.3.

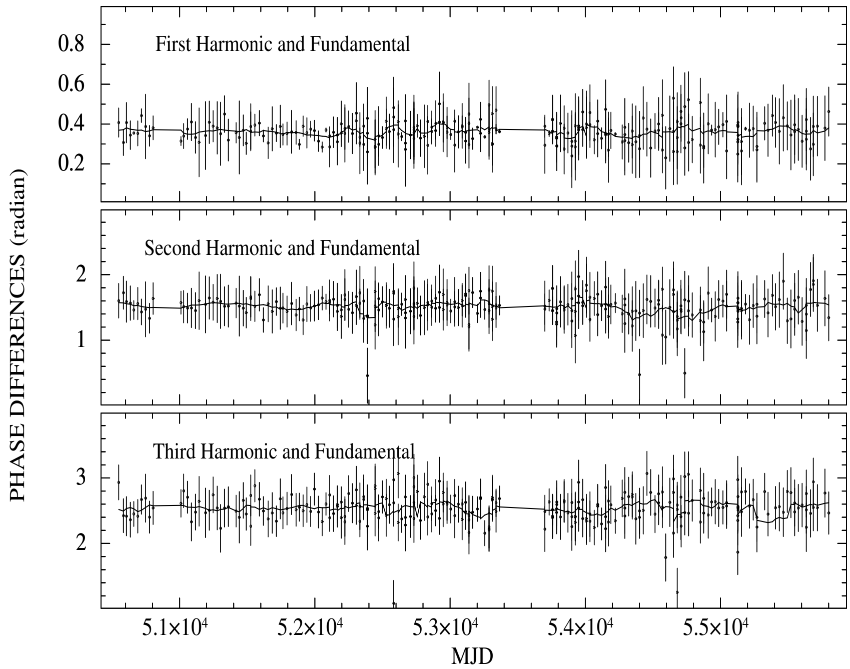

Figure 8.7: The line represents the running mean over nine points of the phase difference of the first three harmonics and the fundamental for the pulse profile of PSR B1509-58 while the points represent the actual values. The X-axis represents the MJD. The error bars are calculated in the same way as Figure 8.6

.

It is worthwhile mentioning that the change in the radio pulse behaviour of pulsars during time as short as their periods is considered a characteristic of radio emission solely. For the rotation powered pulsars, it is not possible to compare single X-ray pulses due to limited photon statistics. However, connection between the spin-down characteristics and the radio emission that is well known, can also be probed for the high energy emission. In this context, it is interesting to note the behaviour of PSR B1931+24. This intermittent pulsar stopped emitting for days during which it spins down half rapidly [451]. For PSR J1841-0500 [452] and PSR J1832+0029 [453] too, changes in spin down rate is associated with the variations in their average radio profiles. For PSR B1509-58, we are investigating if changes in the spin down characteristics are associated with any changes in the high energy emission properties. We have made a quantitative estimate of any possible changes in the pulse profile by carrying out a Fourier decomposition and put upper limits of 36.9 %, 13.4 %, 9.4 % on the amplitudes and 0.36, 1.5, 2.5 radian on the phase of the first three harmonics with respect to the fundamental. A similar study of the pulse profile of the Crab pulsar, but using different analytical expression for the profile, showed no pulse profile variation over a decade [454].

The pulse profile stability of short period X-ray pulsars has an interesting application in interplanetary spacecraft navigation. By comparing the delay between the pulse arrival time measured onboard the spacecraft and the predicted arrival times at an inertial reference like the solar system barycentre, the position information of the spacecraft can be improved along the line of sight towards the pulsar. Three-dimensional position information of the spacecraft can be obtained likewise from the same information of at least three different pulsars [455]. This way, if we have a short period X-ray pulsar with a stable pulse profile, they can be used for navigation of spacecrafts. Also, decomposing the whole pulse profile into its Fourier components as discussed in this work has an advantage over using only the arrival time of the pulse peak [456].

Compared to the millisecond pulsars, PSR B1509-58 is much slower and will not give high position resolution for navigation. However, to be useful for the purpose of navigation, it is necessary for the X-ray pulse profile of rotation powered pulsars to be stable. After the Crab pulsar, PSR B1509-58 is the only bright source with many X-ray observation that can be used to investigate the pulse profile stability. In the present work, we have given upper limits to its profile variation in terms of stability of the harmonic components with respect to the fundamental.